Review

Scanning nonlinear dielectric microscopy

Yasuo Cho[a)]
Research Institute of Electrical Communication, Tohoku University, Aoba-ku, Sendai 980-8577, Japan

(Received 29 March 2011; accepted 21 June 2011)

In this article, scanning nonlinear dielectric microscopy (SNDM) with atomic resolution is reviewed. First, experimental results on the detection of ferroelectric domains are shown following a presentation about the theory and principle of SNDM. Next, a three-dimensional (3D) type of SNDM for measuring the 3D distribution of ferroelectric polarization and noncontact scanning nonlinear dielectric microscopy (NC-SNDM) are proposed. Using NC-SNDM under ultrahigh vacuum conditions, we clearly resolve the electric dipole moment distribution of Si atoms on a Si (111)7 × 7 surface. We also succeeded to resolve a fullerene (C_{60}) molecule. Since the technique is applicable not only to semiconductors but also to both polar and non-polar dielectric materials, $SrTiO_3$ and TiO_2 surfaces were observed by NC-SNDM. Finally, we characterize an ultrahigh-density ferroelectric data storage system using SNDM as a pickup device and a congruent lithium tantalate single crystal as a ferroelectric recording medium.

I. INTRODUCTION

Recently, ferroelectric materials, particularly those in thin-film form, have attracted the attention of many researchers. Their large dielectric constants make them suitable as dielectric layers in microcapacitors in microelectronics. They are also investigated for application in nonvolatile memory using the switchable dielectric polarization of ferroelectric material. To characterize such ferroelectric materials, a high-resolution method is required for observing the microscopic distribution of the remanent (or spontaneous) polarization of ferroelectric materials.

In recent years, we have developed and reported on the use of scanning nonlinear dielectric microscopy (SNDM) for the measurement of the microscopic distribution of dielectric properties on dielectric material surfaces.[1–6]

Another frequently reported high-resolution method used for observing ferroelectric domains is piezoelectric response imaging using scanning force microscopy.[7,8] Compared with this, SNDM is the first successful purely electrical method for observing ferroelectric polarization distribution without the influence of the screening effect from free charges.

Because this microscopic technique has quite a high sensitivity to variation in capacitance, on the order of 10^{-22} F, we have also succeeded in visualizing the electron and hole distributions stored in semiconductor flash memory devices using SNDM.[9–12] Therefore, this technique is expected to be useful for developing new semiconductor devices.

In addition to above-mentioned SNDM techniques, which detects the polarization components perpendicular to the specimen surface only, a new three-dimensional (3D) type of SNDM (3D-SNDM) for measuring the 3D distribution of ferroelectric polarization has been developed.[13–15] Using this 3D-SNDM, it is possible to measure the polarization components both perpendicular (vertical) and parallel (lateral) to the specimen surface by selecting the direction of the applied electric field.

A new technique, noncontact scanning nonlinear dielectric microscopy (NC-SNDM),[16] has been developed to increase the resolution of SNDM. This technique utilizes the signal from higher-order nonlinear dielectric constant ε(4) to control the noncontact state (tip–sample gap control) and simultaneously detect the lowest-order nonlinear dielectric constant ε(3). Thus, NC-SNDM can be used to observe the topography and dielectric properties of materials.

To date, the highest confirmed resolution of SNDM in contact mode operation has been on the subnanometer order of a ferroelectric domain measurement. However, the characterization of the single dipole moment level of a material is expected.

Most recently, we have developed a NC-SNDM system operating in ultrahigh vacuum (UHV) to prove that NC-SNDM has real atomic resolution. Using this microscopic technique, we have succeeded in observing the Si(111)7 × 7 atomic structure.[17,18] We also succeeded to resolve fullerene (C_{60}) molecule.[19] Since the technique is applicable not only to semiconductors but also to both polar and non-polar dielectric materials, $SrTiO_3$ and TiO_2

[a)]Address all correspondence to this author.
e-mail: yasuocho@riec.tohoku.ac.jp
This paper has been selected as an Invited Feature Paper.
DOI: 10.1557/jmr.2011.219

 © Materials Research Society 2011

https://doi.org/10.1557/jmr.2011.219 Published online by Cambridge University Press

surfaces were observed by NC-SNDM. This is the first successful demonstration of the achievement of atomic resolution in a dielectric microscopic technique.

Moreover, we also have proposed a next generation ultrahigh-density ferroelectric data storage system based on SNDM and have already reported that information comprising data bit array of 64 × 64 were successfully stored at an areal density of 4 Tbits/inch^2.[20] These results confirm the potential of ferroelectric materials for storing information at high densities.

In this article, we review and summarize SNDM and its related technologies.

II. PRINCIPLE AND THEORY FOR SNDM AND MICROSCOPIC OBSERVATION OF THE AREA DISTRIBUTION OF FERROELECTRIC DOMAINS USING SNDM

As shown in Fig. 1, we consider the situation where there is a capacitor made of the material to be measured with nonlinearity in D–E relationship and an alternating electric field E_3 along the z-direction (3-direction) is applied to this capacitor. Equation (1) is a polynomial expansion of the electric displacement D_3 as a function of the electric field E_3.

$$D_3 = P_{s3} + \varepsilon(2)E_3 + \frac{1}{2}\varepsilon(3)E_3^2 + \frac{1}{6}\varepsilon(4)E_3^3 + \cdots \quad , \quad (1)$$

where P_{s3} is a spontaneous polarization along the same direction and ε(2), ε(3), and ε(4) are linear, lowest-order nonlinear, and one-order-higher dielectric constants, respectively (The number in the bracket denotes the rank of tensor.).

The even rank tensors, including the linear dielectric constant ε(2), are insensitive to the state of spontaneous polarization. On the other hand, the lowest-order nonlinear dielectric constant ε(3) and other higher-order odd-rank tensor nonlinear dielectric constant are very sensitive to spontaneous polarization. For example, there is no ε(3) in a material with a center of symmetry and the sign of ε(3) changes with the inversion of spontaneous polarization.

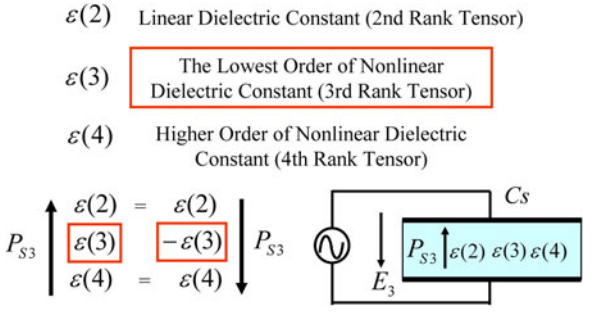


FIG. 1. Principle of polarization detection by scanning nonlinear dielectric microscopy (SNDM).

Therefore, by detecting this ε(3) microscopically, we can measure the distribution of ferroelectric domains.

The capacitance C_s varies alternately owing to the nonlinear dielectric properties of the specimen caused by the application of alternating electric field $E_3 = E_p\cos\omega_p t$. The ratio of the derivative capacitance variation ΔC_s to the static value to the capacitance C_{s0} is given by the following Eq. (2).

$$\frac{\Delta C_S}{C_{S0}} = \frac{\varepsilon(3)}{\varepsilon(2)}E_p\cos\left(\omega_p t\right) + \frac{1}{4}\frac{\varepsilon(4)}{\varepsilon(2)}E_p^2\cos\left(2\omega_p t\right) + \cdots \quad . \quad (2)$$

This equation shows that the alternating capacitance of different frequencies corresponds to each order of the nonlinear dielectric constant. Signals corresponding to ε(3) and ε(4) are obtained by detecting the components with a frequency equal to ω_p and $2\omega_p$ of the applied electric field, respectively.

In the microscopy technique, we have to measure the capacitance variation in the very small portion so that we have developed a special probe for SNDM. Figure 2 shows the system setup of SNDM using an LC lumped constant resonator probe. In the figure, C_s denotes the capacitance of the specimen under the center conductor (the tip) of the probe. C_s is a function of time because of the nonlinear dielectric response under the applied alternating electric field E_{p3} (=$E_p\cos\omega_p t$, f_p = 5 kHz–1 MHz).

This LC resonator is inserted into the positive feedback circuit of a free-running (self-excited) oscillator tuned to the resonance frequency of this resonator. Thus, this oscillator oscillates at the resonance frequency of the LC resonator. The above-mentioned electrical parts [i.e., tip (needle or cantilever), ring, inductance, and oscillator] are assembled into a small probe for the SNDM. The oscillating frequency of the probe (or oscillator) (approximately 1–6 GHz) is modulated by the change in capacitance $\Delta C_s(t)$ due to the nonlinear dielectric response under the applied electric field. As a result, the probe (oscillator) produces a frequency-modulated (FM) signal. By detecting this FM signal using

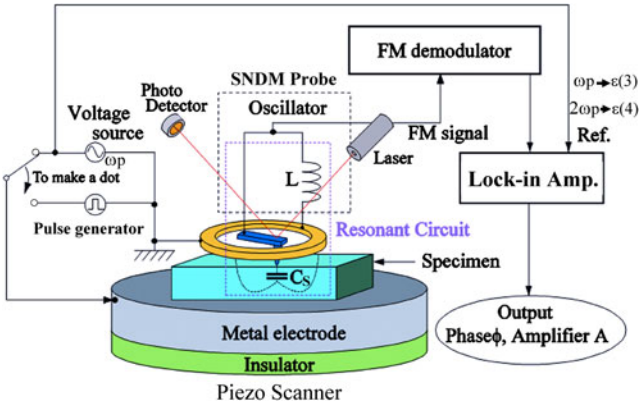


FIG. 2. Schematic diagram of SNDM system.

https://doi.org/10.1557/jmr.2011.219 Published online by Cambridge University Press

the FM demodulator and lock-in amplifier, we obtain a voltage signal proportional to the capacitance variation. Thus, we can detect the nonlinear dielectric constant just under the tip and obtain fine resolution determined by the diameter of the pointed end of the tip and the linear dielectric constant of specimens. The capacitance variation caused by the nonlinear dielectric response is quite small. Therefore, the sensitivity of the SNDM probe must be very high. The measured sensitivity of the above-mentioned lumped constant resonator probe is in the range of 10^{-22} F, which is much higher than that of scanning capacitance microscopy (SCM) whose typical sensitivity is 10^{-18} F.[21]

Originally, SNDM system was developed for the purpose of measuring ferroelectric polarization and local anisotropy of dielectrics through the detection of a third-rank nonlinear dielectric constant.

We performed measurement of a lead zirconate titanate (PZT) film sample using SNDM. The result is shown in Fig. 3. From this image, we can confirm that SNDM can resolve in great detail of a domain structure of PZT. The tip used in this measurement was a metal-coated conductive cantilever with a tip radius of 25 nm. This image is of an epitaxial PZT thin film (400 nm)/La-Sr-Co-O/$SrTiO_3$ substrate.[22] The strip shaped 90° a–c domain pattern is clearly seen in the figure.

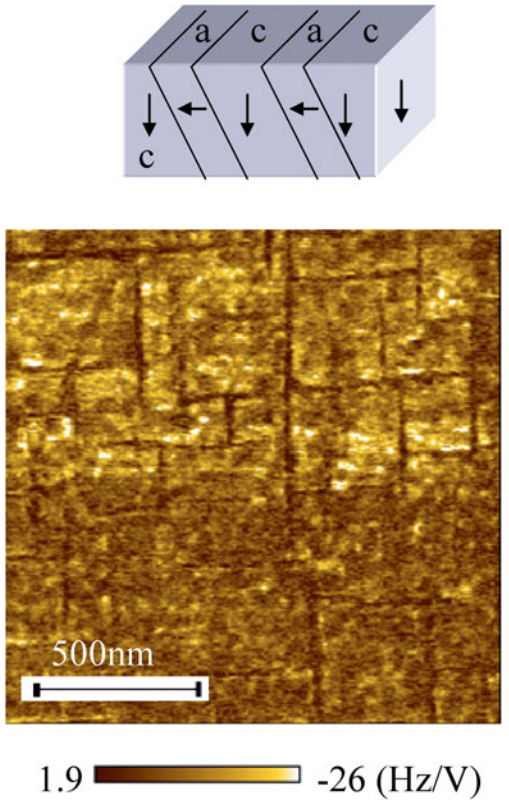


FIG. 3. SNDM image of an epitaxial lead zirconate titanate thin film on La-Sr-Co-O/$SrTiO_3$.

III. SNDM FOR 3D OBSERVATION OF NANOSCALE FERROELECTRIC DOMAINS (3D-SNDM)

The other advantage of SNDM in investigation of ferroelectric materials is that it is possible to measure the polarization components both perpendicular (vertical) and parallel (lateral) to the specimen surface by selecting the direction of the applied electric field.[13–15] The 3D measurement of ferroelectric polarization is quite important because many ferroelectric materials have 3D domain structures.

In ferroelectric materials, the sign of the lowest-order component of the nonlinear dielectric constant (third-rank tensor) changes with an inversion of the polarization direction. Hence, by measuring the sign of the nonlinear dielectric constant, we can obtain the polarization direction. As explained the principle in Fig. 4, in vertical measurement, we apply alternating electric field along the polarization direction and measure the capacitance variation along

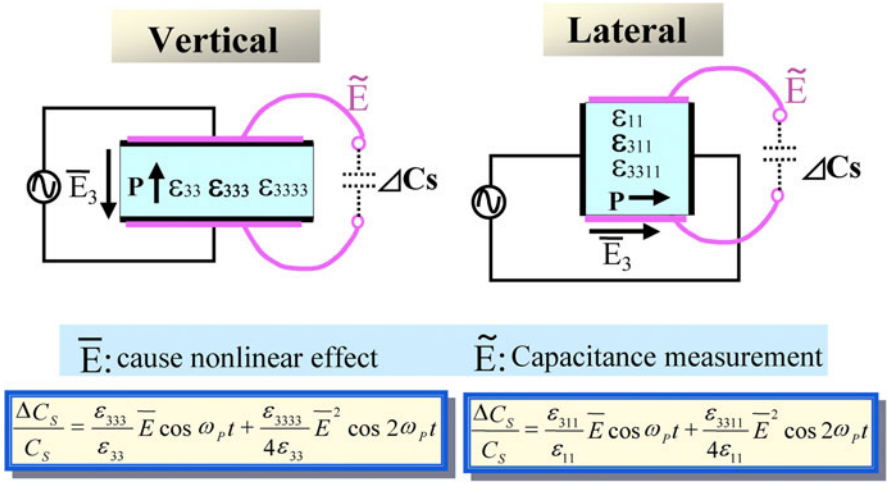


FIG. 4. SNDM principle in vertical and lateral measurements.

https://doi.org/10.1557/jmr.2011.219 Published online by Cambridge University Press

the same direction, thus SNDM detects the component of polarization perpendicular to the specimen surface [ε(3) component]. On the other hand, in lateral measurement, we apply alternating electric field along the polarization direction too; however, we measure the capacitance variation perpendicular to the polarization direction so that it can detect the parallel component polarization (ε_{311} component).

Figure 5 shows a schematic diagram of an SNDM system designed to measure in both the vertical and lateral polarization directions. In vertical measurement, the bottom electrode is used to apply an alternating electric field in the vertical direction. In lateral measurement, an alternating electric field is generated by applying an alternating voltage to four electrodes denoted as A, B, C, and D on the electrode plate. By producing a 90° phase shift between the applied voltages, V_{A-B} ($=2V_1\cos\theta$) and V_{C-D} ($=2V_1\sin\theta$), a rotating electric field is generated parallel to the specimen surface. By using the rotating electric field, the phase output of the lock-in amplifier directly indicates the lateral azimuth angle of polarization.

In this experiment, lateral measurement was carried out in the *x*-cut plane of a multidomain congruent $LiTaO_3$ single crystal with a thickness of 200 μm, which has a lateral polarization component only.

Figure 6(a) shows a phase image obtained for lateral measurement in the *x*-plane of the $LiTaO_3$ crystal. Antiparallel polarization orientations are clearly distinguished in this image. This image further reveals that the c–c domains do not penetrate along the *Z*-axis contrary to the usual expectation, i.e., ferroelectric polarization is expected to penetrate through the crystal along the polarization direction. In other words, the multidomain structure of the congruent $LiTaO_3$ crystal generated by the depolarization process was found to be composed of numerous charged domains. Figure 6(b) also shows a phase image in the x-plane of the $LiTaO_3$ crystal, in which the specimen has been physically rotated by 90°. In these images, where the azimuthal polarization angles are indicated by arrows on the color scale, it can be seen that the phase signals shift by around 90° in accordance with the rotation of the specimen.

IV. NONCONTACT SCANNING NONLINEAR DIELECTRIC MICROSCOPY

Recently, we have developed NC-SNDM operating under UHV conditions.[16] As shown in Fig. 7, NC-SNDM utilizes the signal from higher-order nonlinear dielectric constant ε(4) to control the noncontact state (tip–sample gap control) and simultaneously detect the lowest-order nonlinear dielectric constant ε(3). Thus, NC-SNDM can be used to observe the topography and dielectric properties of materials.

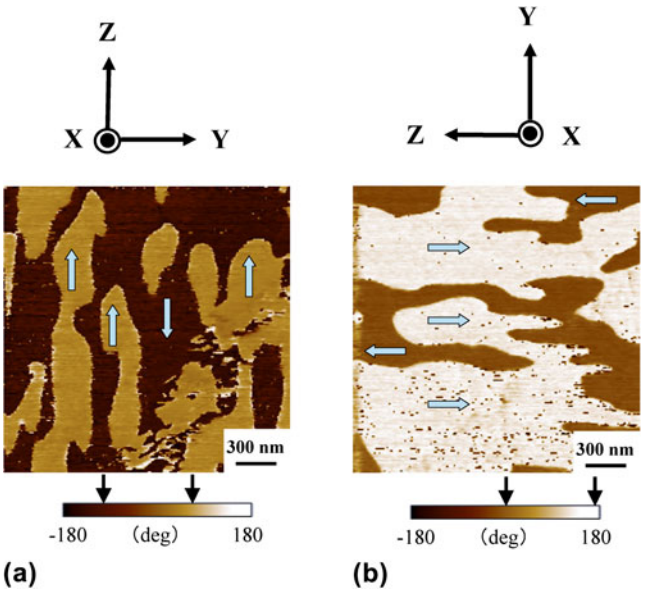


FIG. 6. (a) Phase image in *x*-cut plane of multidomain $LiTaO_3$ substrate by lateral measurement; (b) phase image by lateral measurement after physical rotation of specimen by 90°.

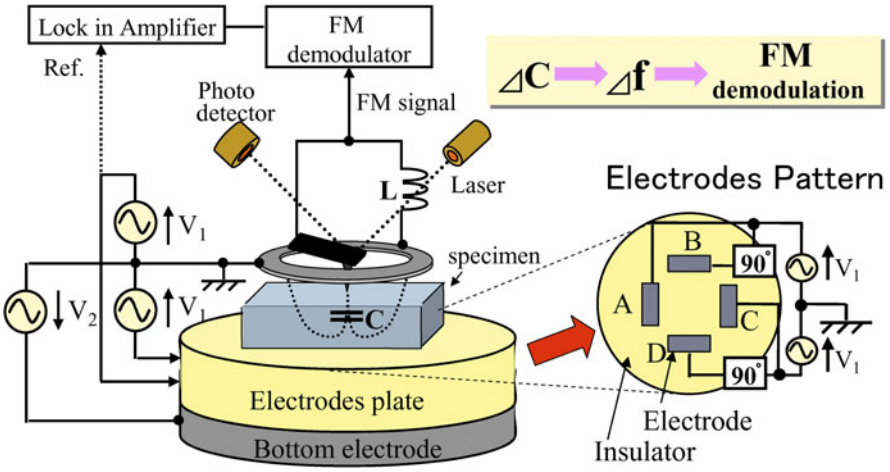


FIG. 5. Schematic diagram of three-dimensional type of SNDM system.

https://doi.org/10.1557/jmr.2011.219 Published online by Cambridge University Press

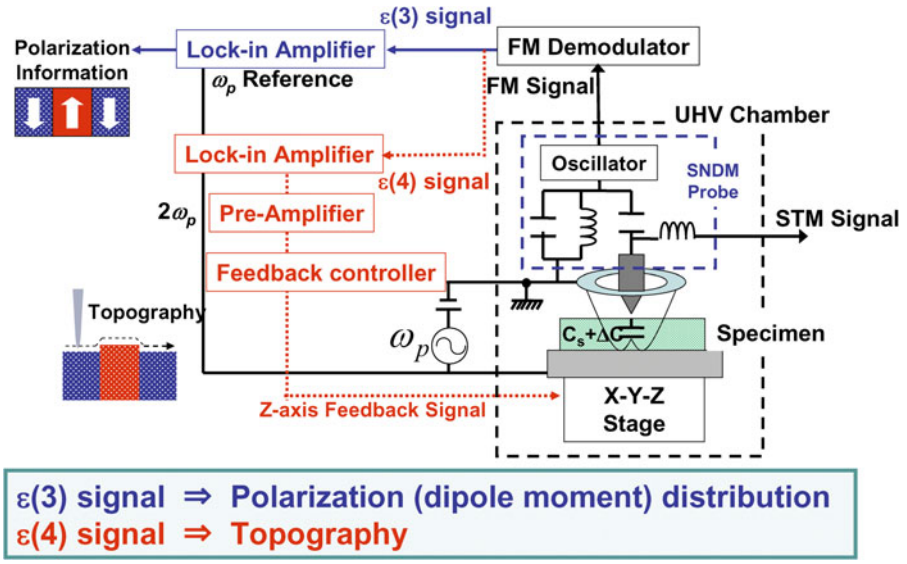


FIG. 7. Brock diagram of noncontact scanning nonlinear dielectric microscopy (NC-SNDM) operated under the ultrahigh vacuum condition.

Equation (2), using the dielectric constant, is a somewhat macroscopic description. However, even if a very localized situation is considered, for example, atomic resolution in mind, because the localized dipole moment also causes capacitance variation, Eq. (2) is still applicable by replacing the macroscopic dielectric constant ε with the local polarizability factor ε_{local} of a single dipole moment as a matter of form.

In the actual measurements, the ambient condition should be UHV because adsorbed water, which has a relatively high-dielectric constant of the order of 80, on the specimen surface causes the electric field under the tip to broaden under such an atmosphere condition.[23] Therefore, an UHV-type SNDM was developed. In this study, the specimen and probe were in a vacuum chamber in which the degree of vacuum was below 1.0×10^{-10} Torr.

To confirm the atomic resolution, a well-established standard sample is required. Therefore, Si(111) was chosen as a representative specimen. In this experiment, an alternating voltage of 3 $V_{p\text{-}p}$ at 30 kHz was applied. Figure 8 shows a simultaneously measured topographical image {image of the height control signal applied to the *Z*-axis piezoscanner to maintain a constant ε_{local} (4) signal [Fig. 8(a)]} and the image of the ε_{local} (3) signal distribution [Fig. 8(b)]. In the topography, the Si(111)7 × 7 atomic structure is clearly recognized; therefore, it is confirmed that the atomic resolution was achieved by NC-SNDM. Moreover, it is also confirmed that the distribution of the ε_{local} (3) signal was obtained simultaneously. Because the ε_{local} (3) image has a contrast that corresponds to individual Si adatoms, this image includes information on the dipole moment of single Si adatoms. This is the first successful demonstration of the achievement of atomic resolution in a dielectric microscopic technique.

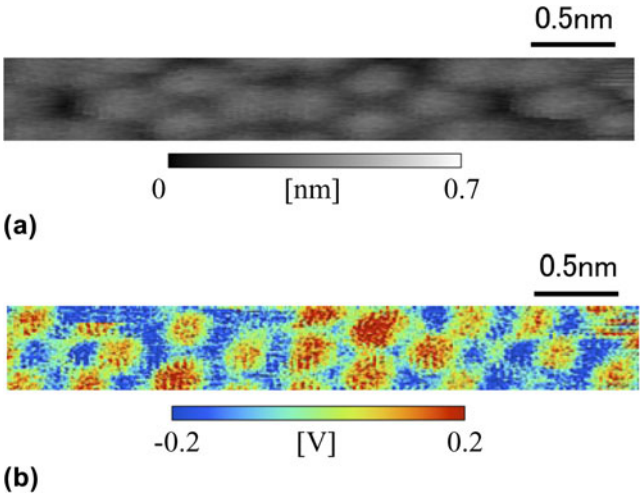


FIG. 8. (a) Topography of Si(111)7 × 7 atomic structure observed by NC-SNDM [ε_{local}(4) feedback]; (b) simultaneously measured dipole moment image by ε_{local}(3) (−0.5 V bias application).

This technique, which is used to detect dielectric properties and topography, is applicable not only to semiconductors but also to both polar and non-polar dielectric materials. Thus, it is expected that NC-SNDM will contribute to the study of electric dipole moment distribution in insulating materials on the atomic level.

We also succeeded to resolve fullerene (C_{60}) molecule deposited on Si(111)7 × 7 surface by NC-SNDM. In this measurement, at first, we fabricated a C_{60} thin film with a thickness of one monolayer on Si(111)7 × 7 surface. The measured result is shown in Fig. 9. This image is an ε(3) ($1\omega_p$) amplitude image with the inset of the expanded image in which the fine internal structure of C_{60} molecule is clearly resolved.

https://doi.org/10.1557/jmr.2011.219 Published online by Cambridge University Press

Next the Si(111)7 × 7 surface covered with 0.37 ML of C_{60} molecules by NC-SNDM is shown in Fig. 10. To obtain the topological image by the NC-SNDM, the ε(4) signal was utilized for the feedback parameter to maintain the gap between the tip of the probe and specimen. The Si(111)7 × 7 surface could be clearly recognized under the C_{60} molecules. The origin of the SNDM signal for the Si(111)7 × 7 surface has been previously reported.[18]

Adsorption site of C_{60} molecules on Si(111)7 × 7 surface was well established by STM.[24,25] For small surface coverage, C_{60} molecules prefer threefold symmetric sites due to the highly symmetric characteristic of C_{60} molecular structure.

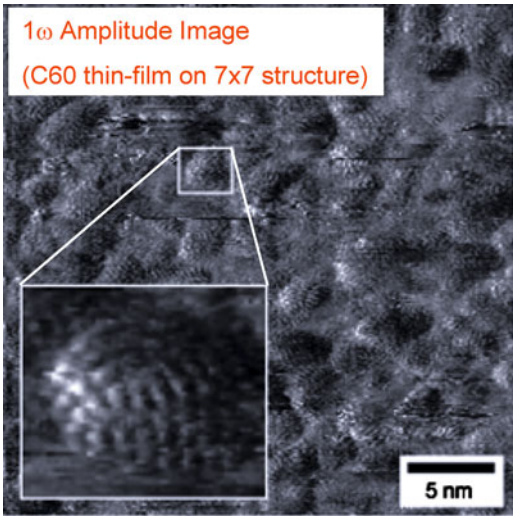


FIG. 9. Internal structure of C_{60} molecule observed by NC-SNDM [ε(3) amplitude image].

Simultaneous phase image of ε(3) (upper left of Fig. 10) and the topography by ε(4) (upper right of Fig. 10) are shown. The tendency of phase reversal can be recognized on almost all the C_{60} molecules, even though phase reversal does not occur on the Si(111)7 × 7 surface.[17,18] The site on the Si(111)7 × 7 surface at which phase reversal occurs was investigated to understand the relationship between the position of the C_{60} molecule and phase reversal. The circles drawn in Fig. 10 correspond to C_{60} molecules where phase reversal did not occur, judging from the unit cell for the Si(111)7 × 7 surface corresponding to the orange dotted triangles drawn in Fig. 10 (upper right). The green circles correspond to C_{60} molecules on the corner holes, whereas the red circles correspond to C_{60} molecules on twofold symmetric sites. The yellow circles correspond to C_{60} molecules whose position cannot be defined due to poor resolution. Surprisingly, no phase reversal for C_{60} molecules on twofold symmetric sites and corner holes can be recognized, and phase reversal only occurred for C_{60} molecules on threefold symmetric sites. This is because the electric dipole moment originating from charge transfer from a Si adatom was only induced on threefold symmetric sites.[19]

Therefore, an electric dipole moment cannot be induced on twofold symmetric sites and corner holes because charge transfer does not occur for C_{60} molecules at these locations.

The ratio of the number of C_{60} molecules on threefold symmetric sites with phase reversal and the total number of C_{60} molecules on twofold symmetric sites and corner holes

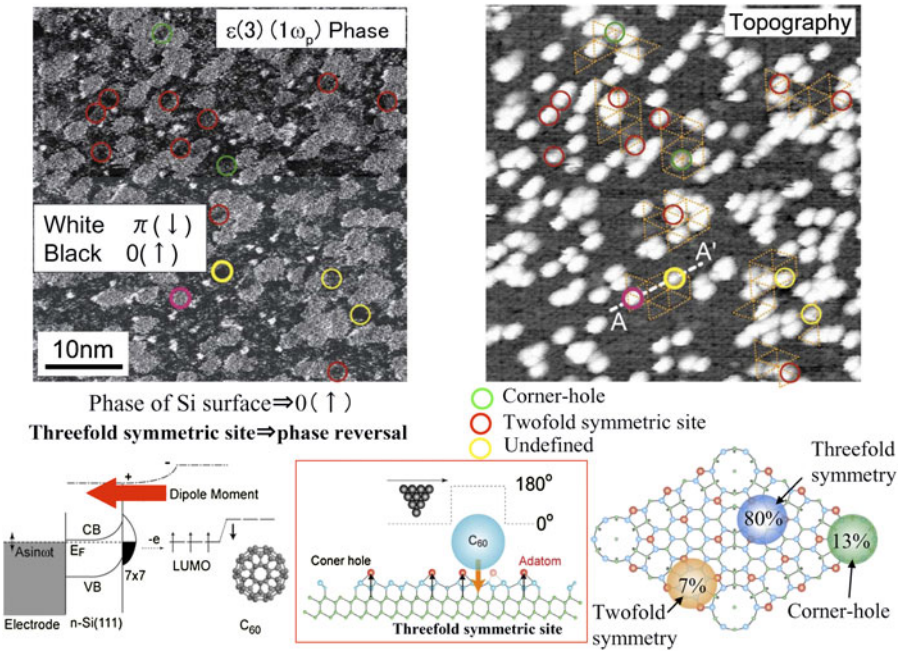


FIG. 10. ε(3) (1ω_p) phase image (upper left) and topography (upper right) by NC-SNDM. Dipole moment induced from C_{60} molecule to threefold symmetric site (lower left and lower middle). Absorption probabilities of C_{60} molecule on Si(111)7 × 7 surface (lower right).

https://doi.org/10.1557/jmr.2011.219 Published online by Cambridge University Press

with no phase reversal is similar to that of the number of C_{60} molecules on the three sites on an Si(111)7 × 7 surface as estimated by STM (as shown in Fig. 10 lower right).[24] Therefore, no phase reversal occurs on the twofold symmetric site and corner hole. Thus, it is considered that the phase of ε(3) signal in NC-SNDM reflects whether an electric dipole moment is induced at the interface between the C_{60} molecule and an individual site.

This means that NC-SNDM can only detect the electric dipole moment induced at the interface between C_{60} molecule and threefold symmetric site.

Since the technique is applicable not only to semiconductors but also to both polar and non-polar dielectric materials, $SrTiO_3$ and TiO_2 surfaces were observed by NC-SNDM. Figures 11(a) and 11(b) show the topography and polarization on Nb-doped $SrTiO_3$(100) surface, respectively. This sample was annealed at 1150 °C for 10 min in UHV condition. In the topography, periodic atomic structure was clearly observed. In the polarization [ε(3)] image, upward polarization was observed. From this result, the surface of this sample is terminated with TiO_2 layer. Next, we also have measured widegap semiconductor TiO_2(100) surface as shown in Fig. 12. This sample was fabricated by heat treatment at 1000 °C for 5 min in UHV condition, too. From the topography [Fig. 12(a)], it is confirmed that one surface structure contains three layers denoted using the symbols XYZ. We think that the microfaceted topography of (110) surface was measured.[26] As shown in the polarization image of Fig. 12(b), upward polarization was detected. We think the signal originates from a Ti cation.

V. NEXT GENERATION ULTRAHIGH-DENSITY FERROELECTRIC DATA STORAGE BASED ON SNDM

With the advances in information processing technology, the importance of high-density data storage is increasing. Studies on thermal fluctuation predict that magnetic storage, which plays a major role in this field,

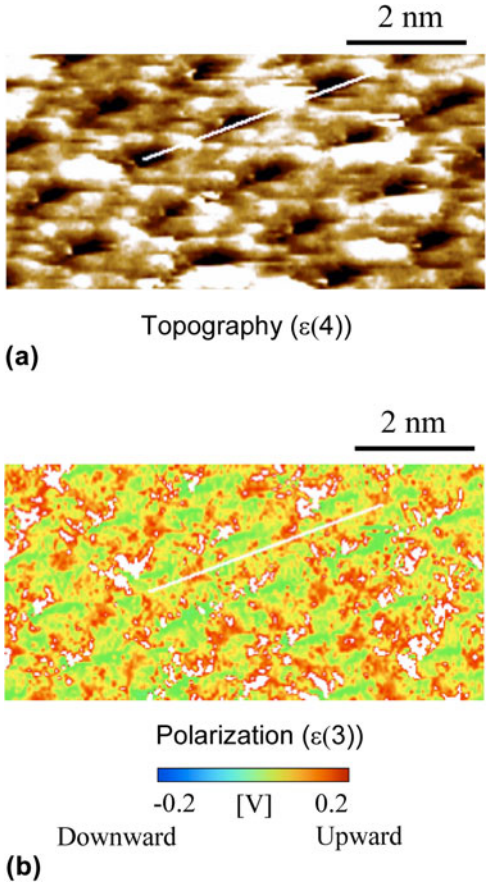


FIG. 11. Topography (a) [ε(4) feedback] and dipole moment (b) [ε(3) image] on Nb-doped $SrTiO_3$(100) surface by NC-SNDM.

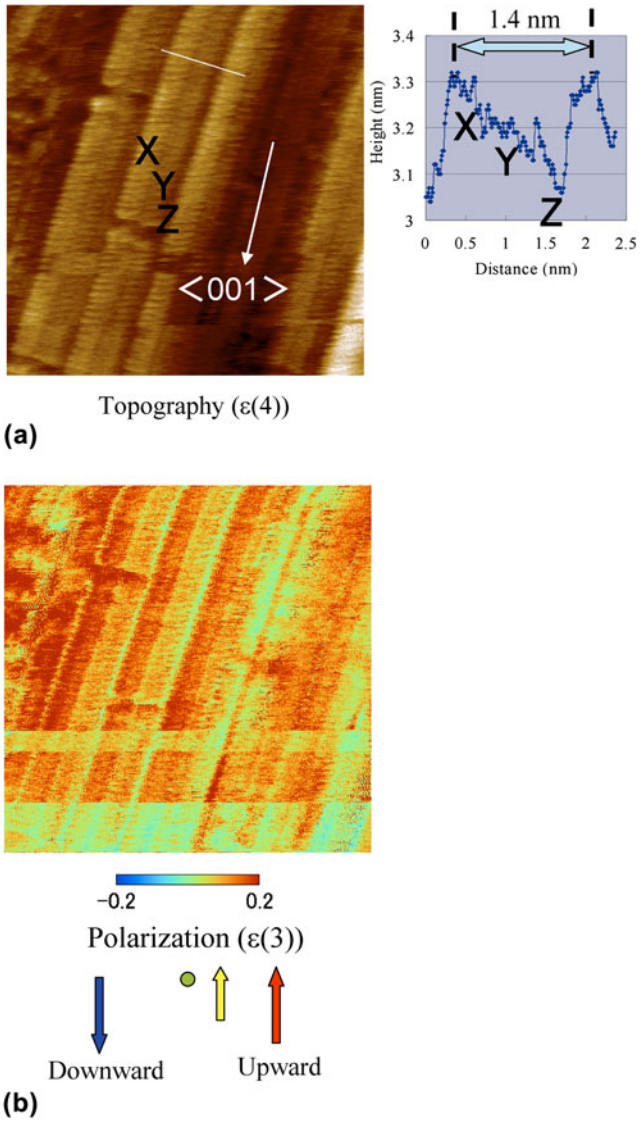


FIG. 12. Topography (a) [ε(4) feedback] and dipole moment (b) [ε(3) image] on widegap semiconductor TiO_2(100) surface by NC-SNDM.

https://doi.org/10.1557/jmr.2011.219 Published online by Cambridge University Press

will reach a theoretical limit in the near future; thus, a novel high-density storage method is required.

Ferroelectrics can hold bit information in the form of the polarization direction of individual domains. Moreover, the domain wall of typical ferroelectric materials is as thin as the order of a few lattices, which is favorable for high-density data storage. Therefore, we have been studying ferroelectric high-density data storage based on SNDM.

In this section, we describe the fundamental studies of artificially formed ferroelectric nanodomains to obtain the information needed for memory applications. First, we investigated how small nanodomain dots were actually formed. As shown in Fig. 13, at this stage, the smallest artificial nanodomain single dot formed was 2.8 nm in diameter.[27] This single dot was formed by the application of an 8.0 V, 10 ns pulse with a direct current offset of 0.5 V on a congruent lithium tantalate (CLT) thin plate with a thickness of 30 nm. If we can form many bits and maintain this domain dot size, the corresponding memory density will reach 82 Tbit/inch^2. However, unfortunately, this goal is somewhat difficult to achieve. When we form bit in the vicinity of another bit, the two bits merge with each other. Therefore, it is very important to evaluate how close domain dots can be formed to each other. We formed a nanodomain dot array composed of bits "1" and "0" varying the bit size and spacing. We then obtained an artificial nanodomain dot array with a bit size of 7 nm as shown in Fig. 14.[27] Because the 7-nm ϕ dots in the array are sufficiently resolvable for practical data storage, it is expected that, with further refinements, the system will be applicable as a storage technology. However, it also should be noted that with the current quality of ferroelectric recording media and the level of technology,these very small domain dots can be formed only in a very small area on the medium. As mentioned above, although we have reported that ferroelectric data storage at a density of above 1 Tbit/inch^2 is possible in principle, this does not necessarily mean that actual information storage, requiring an abundance of bits to be packed together at high density, is easy to achieve. To facilitate actual storage, a large medium of sufficient surface quality and homogeneity is needed. Therefore, demonstration of actual data storage at above 1 Tbit/inch^2 using ferroelectric materials is important to show whether the technology is really achievable. Figure 15 shows an SNDM image of a 64 × 64 data bit array written on a 30-nm-thick CLT recording medium. The data bits of "1" and "0" were recorded as $+z$ and $-z$ domains, respectively. The bit spacing was 12.8 nm, which is equivalent to an areal

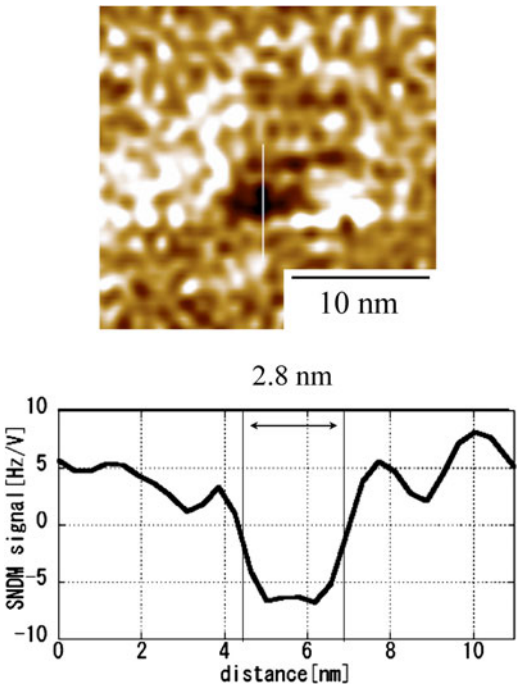


FIG. 13. Smallest artificial nanodomain single dot formed was 2.8 nm in diameter.

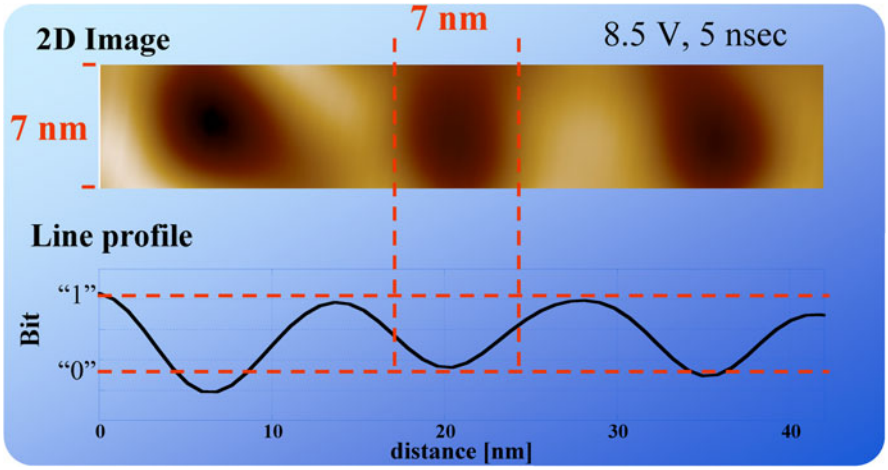


FIG. 14. Artificial nanodomain dot array with a bit spacing of 7 nm formed by 8.5 V, 5 nsec pulses applied with a direct current offset of 0.5 V.

https://doi.org/10.1557/jmr.2011.219 Published online by Cambridge University Press

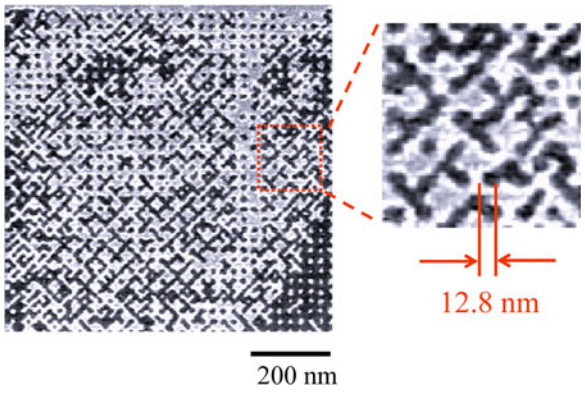


FIG. 15. Actual information recorded at a bit spacing of 12.8 nm (areal recording density: 4 Tbit/inch^2). 64 × 64 bit data written on a congruent lithium tantalate (CLT) single crystal formed on a 30-nm-thick CLT plate.

data storage density of 4 Tbit/inch^2.[20] Thus, real information storage at above 1 Tbit/inch^2 was definitely demonstrated with ferroelectric medium.

VI. CONCLUSIONS

In this article, SNDM with super high resolution was described.

At first, principle and theory for SNDM and microscopic observation of area distribution of ferroelectric domain using SNDM were shown. Then, a new 3D-type of SNDM for measuring the 3D distribution of ferroelectric polarization was developed. Next, NC-SNDM was proposed. Using NC-SNDM, the first achievement of atomic resolution in capacitance measurement was successfully demonstrated. Finally, a very high-density ferroelectric data storage based on SNDM was proposed. Actual visual information data storage at 4 Tbit/inch^2 was successfully demonstrated.

Therefore, we have concluded that the SNDM is very useful for observing ferroelectric nanodomains and the local dipole moment of materials with atomic resolution and has a quite high potential as a nanodomain engineering tool.

REFERENCES

1. Y. Cho, A. Kirihara, and T. Saeki: New microscope for measuring the distribution of nonlinear dielectric properties. *Denshi Joho Tsushin Gakkai Ronbunshi* **J78-C-1**, 593 (1995) [in Japanese].
2. Y. Cho, A. Kirihara, and T. Saeki: Scanning nonlinear dielectric microscope. *Rev. Sci. Instrum.* **67**, 2297 (1996).
3. Y. Cho, S. Atsumi, and K. Nakamura: Scanning nonlinear dielectric microscope using a lumped constant resonator probe and its application to investigation of ferroelectric polarization distributions. *Jpn. J. Appl. Phys.* **36**, 3152 (1997).
4. Y. Cho, S. Kazuta, and K. Matsuura: Scanning nonlinear dielectric microscopy with nanometer resolution. *Appl. Phys. Lett.* **72**, 2833 (1999).
5. H. Odagawa and Y. Cho: Simultaneous observation of nanosized ferroelectric domains and surface morphology using scanning nonlinear dielectric microscopy. *Surf. Sci.* **463**, L621 (2000).
6. T. Morita and Y. Cho: Piezoelectric performance and domain structure of epitaxial $PbTiO_3$ thin film deposited by hydrothermal method. *Jpn. J. Appl. Phys.* **45**, 4489 (2006).
7. A. Gruverman, O. Auciello, R. Ramesh, and H. Tokumoto: Scanning force microscopy of domain structure in ferroelectric thin films: Imaging and control. *Nanotechnology* **8**, A38 (1997).
8. L.M. Eng, H.-J. Güntherodt, G.A. Schneider, U. Köpke, and J.M. Saldaña: Nanoscale reconstruction of surface crystallography from three-dimensional polarization distribution in ferroelectric barium–titanate ceramics. *Appl. Phys. Lett.* **74**, 223 (1999).
9. K. Honda and Y. Cho: Visualization using scanning nonlinear dielectric microscopy of electrons and holes localized in the thin gate film of a metal–SiO_2–Si_3N_4–SiO_2–semiconductor flash memory. *Appl. Phys. Lett.* **86**, 013501 (2005).
10. K. Honda, S. Hashimoto, and Y. Cho: Visualization of electrons and holes localized in the thin gate film of metal SiO_2-Si_3N_4-SiO_2 semiconductor type flash memory using scanning nonlinear dielectric microscopy after writing-erasing cycling. *Appl. Phys. Lett.* **86**, 063515 (2005).
11. K. Honda, S. Hashimoto, and Y. Cho: Visualization of electrons and holes localized in the thin gate film of metal-oxide-nitride-oxide-semiconductor type flash memory by scanning nonlinear dielectric microscopy. *Nanotechnology* **16**, 90 (2005).
12. K. Honda, S. Hashimoto, and Y. Cho: Visualization of charges stored in the floating gate of flash memory by scanning nonlinear dielectric microscopy. *Nanotechnology* **17**, S185 (2006).
13. H. Odagawa and Y. Cho: Measuring ferroelectric polarization component parallel to the surface by scanning nonlinear dielectric microscopy. *Appl. Phys. Lett.* **80**, 2159 (2002).
14. T. Sugihara, H. Odagawa, and Y. Cho: Three-dimensional measurement for absolute value of polarization angle by scanning nonlinear dielectric microscopy. *Jpn. J. Appl. Phys.* **44**, 4325 (2005).
15. T. Sugihara and Y. Cho: Three-dimensional observation of nanoscale ferroelectric domains using scanning nonlinear dielectric microscopy with electric field correction by Kelvin probe force microscopy. *Nanotechnology* **17**, S162 (2006).
16. K. Ohara and Y. Cho: Non-contact scanning nonlinear dielectric microscopy. *Nanotechnology* **16**, 54 (2005).
17. R. Hirose, K. Ohara, and Y. Cho: Observation of the Si(111)7×7 atomic structure using non-contact scanning nonlinear dielectric microscopy. *Nanotechnology* **18**, 084014 (2007).
18. Y. Cho and R. Hirose: Atomic dipole moment distribution of Si atoms on a Si(111)-(7×7) surface studied using noncontact scanning nonlinear dielectric microscopy. *Phys. Rev. Lett.* **99**, 186101 (2007).
19. S. Kobayashi, and Y. Cho: Investigation of interface between fullerene molecule and Si(111)-7×7 surface by noncontact scanning nonlinear dielectric microscopy. *J. Vac. Sci. Technol. B* **28**, C4D18 (2010).
20. K. Tanaka and Y. Cho: Actual information storage with a recording density of 4 Tbit/in.^{2} in a ferroelectric recording medium. *Appl. Phys. Lett.* **97**, 092901 (2010).
21. Y. Nakagawa: Scanning capacitance microscope, in *Roadmap of Scanning Probe Microscopy*, edited by S. Morita (Springer, New York, 2006) pp. 35, 42.
22. C.S. Ganpule, V. Nagarajan, H. Li, A.S. Ogale, D.E. Steinhauer, S. Aggarwal, E. Williams, R. Ramesh, and P. De Wolf: Role of 90° domains in lead zirconate titanate thin films. *Appl. Phys. Lett.* **77**, 292 (2000).

https://doi.org/10.1557/jmr.2011.219 Published online by Cambridge University Press

23. K. Ohara and Y. Cho: Effect of the surface adsorbed water on the studying of ferroelectrics by scanning nonlinear dielectric microscopy. *J. Appl. Phys.* **96**, 7460 (2004).
24. X.D. Wang, T. Hashizume, H. Shinohara, Y. Saito, Y. Nishina, and T. Sakurai: Scanning tunneling microscopy of C_{60} on the Si(111) 7x7 surface. *Jpn. J. Appl. Phys.* **31**, L983 (1992).
25. J.G. Hou, Y. Jinlong, W. Haiqian, L. Qunxiang, Z. Chanhhan, L. Hai, B. Wang, D.M. Chen, and Z. Qingshi: Identifying molecular orientation of individual C_{60} on a Si(111)-(7 $\times$ 7) surface. *Phys. Rev. Lett.* **83**, 3001 (1999).
26. P.J. Hardman, N.S. Parkash, C.A. Muryn, G.N. Raikar, A.G. Thomas, A.F. Prime, G. Thornton, and R.J. Blake: Oxgen-vacancy sites on TiO_2(100)1x3 using surface core-level-shift photoelectron diffraction. *Phys. Rev. B* **47**, 16056 (1993).
27. K. Tanaka, Y. Kurihashi, T. Uda, Y. Daimon, N. Odagawa, R. Hirose, Y. Hiranaga, and Y. Cho: Scanning nonlinear dielectric microscopy nano-science and technology for next generation high density ferroelectric data storage. *Jpn. J. Appl. Phys.* **47**, 3311 (2008).

https://doi.org/10.1557/jmr.2011.219 Published online by Cambridge University Press